

ORIGINAL RESEARCH PAPER

# Optimization of Superimposed Residual Stress Components to Improve Fatigue Life of Work Roll in Hot Rolling Process Using Artificial Neural Network and Genetic Algorithm

B. Salehebrahimnejad<sup>a</sup>, A. Doniavi<sup>a</sup>, M. Moradi<sup>b</sup>, M. Shahbaz<sup>c,\*</sup>

<sup>a</sup>Department of Mechanical Engineering, Faculty of Engineering, Urmia University, Urmia, Iran.

<sup>b</sup>Department of Mechanical Engineering, Isfahan University of Technology, Isfahan, Iran.

<sup>c</sup>Department of Materials Science and Engineering, Faculty of Engineering, Urmia University, Urmia, Iran.

## Article info

### Article history:

Received 15 February 2022

Received in revised form

08 March 2022

Accepted 15 March 2022

### Keywords:

Residual stress

Von-Mises stress

Design of experiment

Artificial neural network

Genetic algorithm

Optimization

Hot rolling

## Abstract

In this paper, a semi-analytical model was proposed to superimpose the initial residual stress components on the work roll surface and subsurface to minimize the maximum value of Von-Mises Stresses (MVMS) during the hot rolling process to reduce the possibility of roll wear and increase the fatigue life. A Finite Element Model (FEM) was proposed to assess the temperature and thermomechanical stress in work roll during hot rolling. An analytical method was developed to implement the three initial residual stress components designed by the full factorial analysis of variance (ANOVA) method in the obtained FEM thermomechanical stress results. An Artificial Neural Network (ANN) was used to establish an objective function to relate the initial residual stress components to the MVMS. Subsequently, the single and multi-objective Genetic Algorithm (GA) optimization were used to find the optimal value of initial residual stress components to minimize the MVMS on the surface and subsurface of the work roll. The results showed a significant reduction of both the value and amplitude of the MVMS on surface and subsurface of a work roll during the hot rolling process.

## 1. Introduction

The surface layers of work rolls in the hot rolling industrial process are commonly imposed to cyclic thermal and mechanical stresses during their service life. These cyclic stresses in macro-scale and micro-scale lead to localized micro-scale plastic deformation and damage accumulation on the work roll surface in roughing trains and finishing stands [1–3]. These damages are related to fatigue cracks that nucleate and grow under thermal and mechanical cyclic stresses [4]. Therefore, there is a

strong relationship between the surface wear rate and the plastic deformation [5]. Since the onset of plastic deformation is governed by MVMS, this criterion is an excellent indicator of the effectiveness of all stress tensor components on the fatigue life [6–8].

It can be stated that one way to suppress or delay the plastic strain is to reduce the MVMS stress [3, 6–8]. A few investigators have presented that this aim can be achieved by incorporating a shallow surface layer of compressive residual stress [9–11]. In a contrary viewpoint, if the combination of compressive residual stress

\*Corresponding author: M. Shahbaz (Assistant Professor)

E-mail address: m.shahbaz@urmia.ac.ir

<http://dx.doi.org/10.22084/jrstan.2022.26129.1209>

ISSN: 2588-2597

and in-service stress exceeds the compressive yield limit of the roll material, the roll surface will deform plastically, and crack nucleation will begin [1]. Therefore, there remains a need for an optimum value of compressive residual stress that can balance these two tendencies and improves the rolling fatigue life. For example, Cretu et al. [12] used an equivalent critical stress criterion for finding the optimum residual stress distribution with an experimentally confirmed positive effect on the fatigue life of ball bearing. Warhadpande et al. [8] studied the influence of superimposed residual stress patterns on the MVMS of bearing operation by a 2-D elasto-plastic FEM model. Recently, Mahdavi et al. introduced a 2-D elastic semi-analytical framework [3] and an elastoplastic micromechanical model [13] to evaluate a favorable macro-scale compressive residual stress in the vicinity of non-metallic inclusion and related it to the micro-scale Von-Mises stress as the optimization criterion of fatigue initiation. However, although the effect of initial compressive residual stress on the mechanical fatigue life of bearings was demonstrated over time, little attention has been paid to the effect of initial compressive residual stress on the thermal and mechanical fatigue life of work rolls in hot rolling operation. Moreover, there is no study to consider the effect of each independent component of residual stress on the rolling fatigue life separately.

This study represents a semi-analytical model to generate three components of stress tensors as initial compressive residual stresses in surface and subsurface layers of FEM of hot rolling work roll to minimize the MVMS. The ANOVA with full factorial experiments is employed to obtain enough data for establishing an objective function by ANN. ANN was used to create the mathematical relationship between input initial residual stresses and the MVMS in different layers using Matlab software. Moreover, the model was applied to determine the optimum value of each component of initial residual stress by single-objective and multi-objective GA to achieve the minimum value of MVMS as a means for suppressing or delaying the onset of plasticity and increasing the roll fatigue life.

## 2. Theory

### 2.1. Finite Element Analysis

According to the previous finite element analysis (FEA) of the hot rolling work roll in three-dimensional (3D) [14, 15] and two-dimensional (2D) [16–19], a 2D plane-strain FEM of only rotating work roll and fixed boundary conditions is used here in order to study temperature and thermo-mechanical stress evolution of work roll during hot rolling process. The advantage of 2D over 3D FEM is a reduction of total computational effort and time. The elastic FEA was developed using ABAQUS/Standard commercial finite element solver

(Fig. 1a) [20]. The linear elasticity of the model is a conservative constraint for excluding cyclic plasticity [3]. A local cylindrical coordinate system is defined such that radial direction is along the X-direction, tangential direction along the Y-axis, and axial direction along the Z-axis as shown in Fig. 1a. As detailed in this Fig. 1, mesh refinement is positioned near-surface in order to improve the calculation accuracy, and coarse mesh was used inside the work roll to reduce the total computation effort and time. The mesh size was selected to be independent of temperature and stress results. In the center of the model, a reference point was placed and coupled to the surface points of the small hole to conduct a circular motion. This model is based on the experimental work done for on-site measurement of the temperature change in an S.G. cast iron work roll in a roughing stand of a medium-width strip mill [2]. Fig. 1b shows the detailed boundary conditions along the circumferential direction of the work roll, where four regions were divided. Region AB involves the roll bite region, regions BC and DA indicate the natural air cooling regions, and region CD indicates the nozzle-spraying region. During the FEA, the convective heat transfer coefficients in nozzle spraying and natural air-cooling regions were defined in a user subroutine film [20]. Roll bite region subjected to constant heat flux and rolling pressure using Dflux subroutine and Dload subroutine, respectively [20].

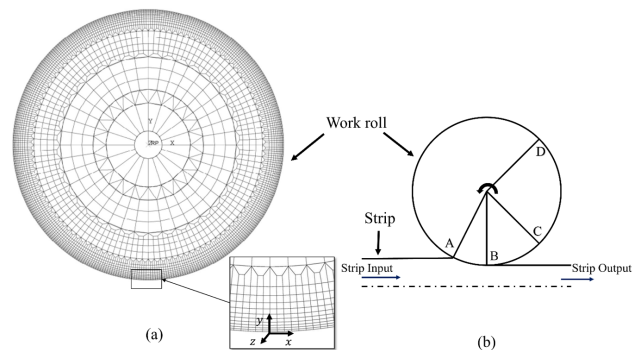


**Fig. 1.** FEM model of the S.G. cast iron work roll: a) Circumferential plane of FEA model with detailed mesh; b) Schematic of boundary condition during hot rolling.

The rolling parameters and physical and mechanical properties of work roll and strip are shown in Tables 1 and 2, respectively. The heat transfer coefficients in the air cooling and nozzle-spraying regions were calculated based on the formula used in [10]. Also, input thermal flux was calculated by the equation proposed by Deng et al. [18]. An equation developed by Shida [21] for hot-rolled strip flow stress was considered to generate the rolling pressure based on the well-known expression developed by Sims [22]. The deformation conditions needed for calculating the Shida's flow stress, such as the rolling reduction and temperature of the strip, are detailed in Table 1.

**Table 1**

Rolling parameters of the work roll and hot strip used in the simulation.

| Parameters                                       | Value  |
|--|--|
| Velocity of the work roll (rad/s) [2]            | 1.31   |
| Roll diameter (mm) [2]                           | 800  |
| Initial work roll temperature (K) [2]            | 293.15   |
| Entry strip temperature (K) [2]                  | 1503.15  |
| Air/Water temperature (K) [2]                    | 293.15   |
| Entry strip width (m)                            | 1  |
| Rolling reduction (%) [2]                        | 22.5%  |
| Rolling pressure (MPa)                           | 63.3   |
| Heat transfer coefficient (W/(m <sup>2</sup> K)) | Bite region, 18000 [2] Water cooling, 35000 [10] Air cooling, 5 [10]               |
| Sectors (degree)                                 | Heating (AB), 13 Air cooling (BC), 12 Water cooling (CD), 97 Air cooling (DA), 238 |

The Steel St37-2 was considered as the strip material with carbon content equal to 0.032%. The sticking friction was considered to model the contact arc between the hot-rolled strip and work rolls. The element used in the analysis is four-node plain strain thermally coupled quadrilateral CPE4T with bilinear displacement and temperature.

**Table 2**

Mechanical and thermal properties of work roll material.

| Parameters                              | Value                   |
|---|-------------------------|
| Young's modulus (GPa) [2]               | 175                     |
| Poisson's ratio [2]                     | 0.275                   |
| Density (kg/m <sup>3</sup> ) [2]        | 7800                    |
| Thermal expansion coefficient (1/K) [2] | 12.6 × 10 <sup>-6</sup> |
| Thermal conductivity (W/(m K)) [2]      | 35                      |
| Specific heat (J/(kg K)) [18]           | 460                     |

## 2.2. Analytical Model

Let  $\sigma_{kl}(y, t)$  be the original stress tensor depending on the local depth  $y$  (see Fig. 1a, detailed section) and rolling time  $t$  extracted from FEA results at each arbitrary point. Based on the linear elasticity, the MVMS can be considered a valid criterion for suppressing micro-scale plasticity entirely [6–8]. In this linear mapping, the offset stress state  $\hat{\sigma}_{kl}(y, t, \sigma_{res}(y))$  replacing the original one  $\sigma_{kl}$  at each specific point can be represented by the following combination with the superimposed residual stress state  $\sigma_{res}$ :

$$\hat{\sigma}_{kl}(y, t, \sigma_{res}(y)) = \sigma_{kl}(y, t) + \begin{bmatrix} \sigma_{11,res}(y) & 0 & 0 \\ 0 & \sigma_{22,res}(y) & 0 \\ 0 & 0 & \sigma_{33,res}(y) \end{bmatrix} \quad (1)$$

The pattern of arbitrary initial residual stress in three directions can be accounted for through modification of Eq. (1). This modification resulted in the

following Von-Mises stress formula:

$$\sigma_{VM}(y, t, \sigma_{res}(y)) = \sqrt{\frac{(\hat{\sigma}_{11} - \hat{\sigma}_{22})^2 + (\hat{\sigma}_{33} - \hat{\sigma}_{11})^2 + (\hat{\sigma}_{22} - \hat{\sigma}_{33})^2 + 6\hat{\sigma}_{12}^2}{2}} \quad (2)$$

The idea is to minimize the MVMS at each depth by finding an optimum value of each component of initial residual stress resulting in maximum fatigue life of work roll during hot rolling.

## 2.3. Optimization

ANN is used here to map the data set of three input variables and a set of targets. The radial, axial, and tangential residual stress components were considered input variables. Full factorial ANOVA designs were utilized to create enough data set at three depths in six levels of residual stress components, as shown in Table 3. By conducting a full factorial analysis using Minitab software, 216 data sets were designed by combining three input variables at different levels. Therefore, each data set was determined by changing input variables in six levels. The amount of upper and lower bound of the residual stress interval was obtained based on the pre-simulation and experimental observations of maximum initial compressive residual stress after the heat treatment process in related literatures [23–25]. The targets were calculated by superimposing the designed input data set into the attained finite element simulated stress through Eq. (1). This can lead to the new Von-Mises stresses as the output variables through Eq. (2). For the training of the ANN, we used the Matlab Neural Networks module. The network is a two-layer feedforward network with a sigmoid transfer function in the hidden layer and a linear transfer function in the output layer. The data set was randomly divided for each combination of state, input, and output variables into training (70%, 152 samples), validation (15%, 32 samples), and test set (15%, 32 samples).

**Table 3**  
Input parameters and their levels.

| Parameter                                   | Level |     |     |     |     |     |
|---|-------|-----|-----|-----|-----|-----|
|   | 1     | 2   | 3   | 4   | 5   | 6   |
| Initial compressive radial stress (MPa)     |       |     |     |     |     |     |
| Initial compressive tangential stress (MPa) | 0     | 130 | 260 | 390 | 520 | 650 |
| Initial compressive axial stress (MPa)      |       |     |     |     |     |     |

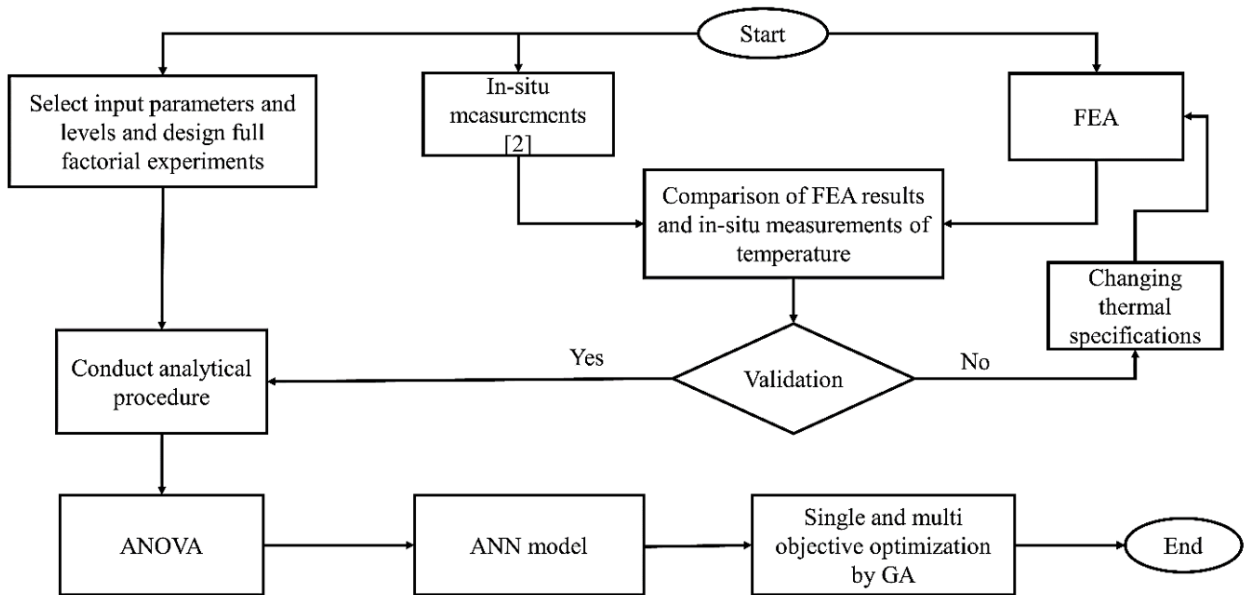


**Fig. 2.** The flowchart of considered steps in this study.

For the training, the Bayesian regularization back-propagation algorithm was used. The network structure consists of one hidden layer with 20 neurons. The number of neurons was selected based on the minimum value of the test and training mean-square-error (MSE) in an iterative trial-and-error procedure. The epoch number was 1000, and the training finished after 1000 iterations. The measurement of the performance of the ANN model is done by using the MSE and coefficient of correlation (R). The MSE and R values of the test network are 0.134 and 0.99998 on the surface, 0.478 and 0.99994 at a depth of 1.7mm, and 0.255 and 0.9994 at a depth of 3.5mm, respectively. According to these results, we can say that the ANN is very well at predicting the MVMS. After fitting the data, neural network function was generated that forms a generalization of the input-output relationship. The attained fitness function was implemented into the Matlab optimization toolbox as an objective function. The lower and upper bounds on the input variables are determined based on Table 3. Then, GA solver was used to find a minimum value of the objective function on the surface and selected depths. Fig. 2 shows the flowchart of considered steps in this study.

### 3. Results and Discussion

#### 3.1. Temperature Variations

Fig. 3a compares simulated and experimental results of reference [2] during the first revolution. The simulation results agree with the experimental on-site measurement that indicates the reliability of the FEA of the S.G cast iron work roll during hot rolling. As can be seen, the surface temperature increases rapidly from 20°C to 534°C during contact with the hot strip (AB). It then decreases due to subsequent air cooling (BC) and water cooling (CD) until reaching a stable value of 50°C. After the water-cooling position (point D) had been passed, the surface temperature increased slightly due to heat conduction from subsurface layers of a higher temperature. This is consistent with results obtained in previous studies [16–19]. The variation of the simulated roll temperature history of three-selected depths during the five revolutions is shown in Fig. 3b. As can be seen, the maximum temperature increases gradually on the surface during the first three revolutions. It then reaches a stable maximum value of about 545°C during subsequent revolutions.

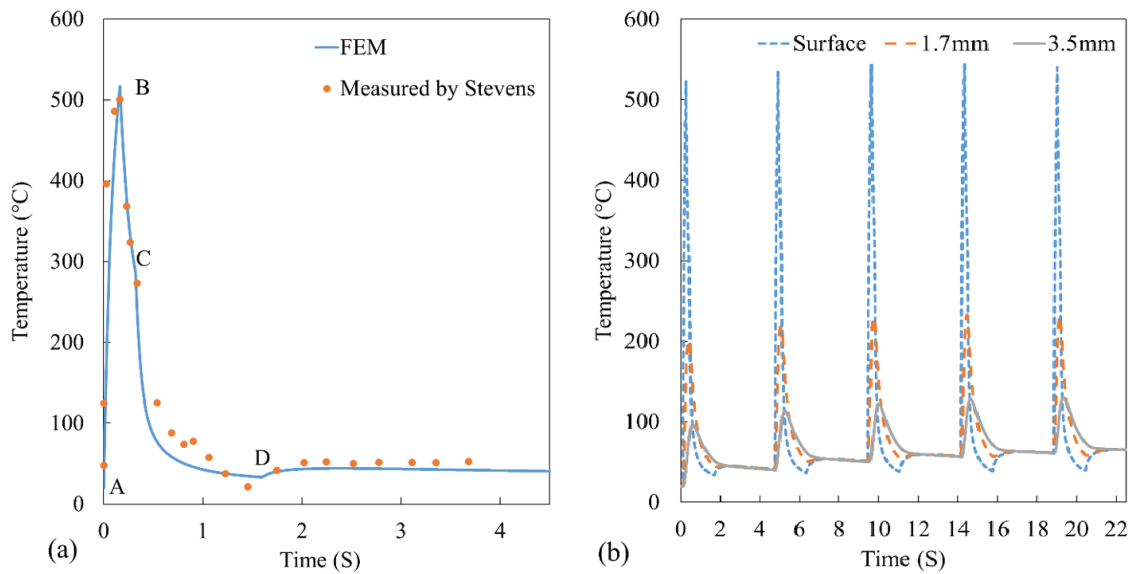


**Fig. 3.** a) Verifying simulated temperature by Stevens on-situ measurements [2]; b) Temperature histories of three selected depths during the early five revolutions from FEA.

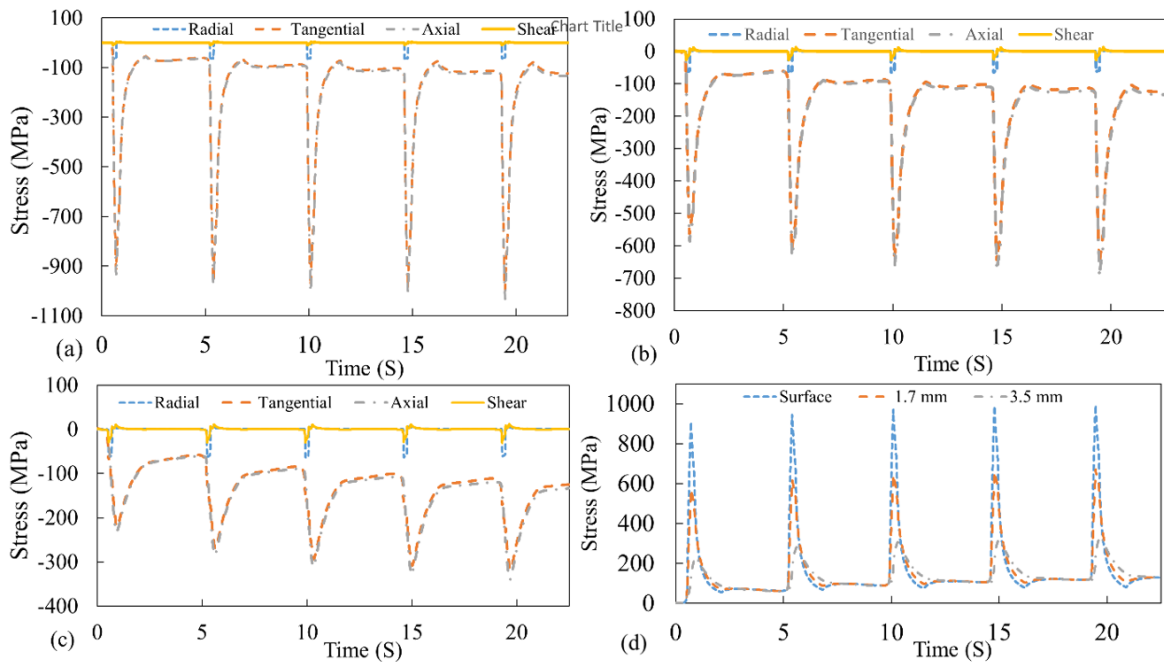


**Fig. 4.** a) Stress components evolution history at roll surface; b) Stress components evolution history at 1.7mm beneath the surface; c) Stress components evolution history at 3.5mm beneath the surface; d) Von-Mises stress within different depths.

Also, it can be stated that there is no stable maximum temperature beneath the surface during early revolutions due to non-uniform conduction between different depths. The maximum temperature at depths of 1.7mm and 3.5mm during the early five revolutions are equal to 233°C and 130°C, respectively, which are significantly lower than the surface temperature. Therefore, it can be concluded that the extreme temperature is limited to a thin surface layer only.

### 3.2. Thermo-mechanical Stresses

Fig. 4 illustrates all relevant thermo-mechanical stress profiles on the surface, 1.7mm and 3.5mm beneath the surface. As can be seen, axial and tangential stress distributions are almost identical, and a minimum value of radial stress is due to rolling pressure. Fig. 4a illustrates the maximum compressive axial and tangential stresses of 933 and 914MPa, respectively. They developed on the roll surface due to contact with the

hot strip in the first revolution, then reached a stable value of about 1033MPa in axial direction and 999MPa in tangential directions in subsequent revolutions. At a depth of 1.7mm (see Fig. 4b), the maximum compressive axial and tangential stresses in the first revolution reduced to 585 and 562MPa, respectively. This reduction of the maximum compressive axial and tangential stresses in the first revolution continues to 231 and 220MPa at the depth of 3.5mm, as shown in Fig. 4c. As can be seen, there was no stable compressive stress at these depths during the early five revolutions. A comparison with temperature variations in Fig. 3 confirms that the stresses at the depths of 1.7mm and 3.5mm follow a similar pattern to the temperature variations. Fig. 4d shows that Von-Mises stress on the surface when the first revolution reaches 909MPa and is then reduced to 50MPa during subsequent cooling, which shows a significant amplitude level. In the subsequent revolutions, the Von-Mises stress gets a stable amplitude between 994MPa and 63MPa. In addition, it can be concluded that there are much smaller Von-Mises stresses at selected depths than on the surface. Thus, a significant Von-Mises stress develops on the roll surface, where the material undergoes plastic deformation. So, the voids and cracks initiate and grow toward the depth [2]. Regarding the effect of high-magnitude of Von-Mises stress, it is apparent that high-stress amplitude also leads to a significant reduction in the fatigue life due to an increase in the growth rate of short cracks on the surface [25]. Therefore, it can be concluded that minimizing the MVMS by superimposing the optimal residual stresses is beneficial in improving the fatigue life.

### 3.3. Optimization

The input parameters determined in section 2.3 was applied to FEA simulated results of three directions at three depths in order to minimize the maximum value of attained Von-Mises stresses. Table 4 depicts the optimal residual stresses required for maximum reduction in Von-Mises stress at three depths obtained by the ANN method and GA optimization. A summary of the ANOVA result is given in Table 5. All input parameters and interactions were highly significant ( $P < 0.001$ ). The results illustrate that the initial radial stress has the most effect on the Von-Mises stress, with the contribution of 63.7% on the surface, 55.1% at the depth of 1.7mm, and 24.8% at the depth of 3.5mm. The contributions of the tangential and the axial stress are 14.8% and 18.1% on the surface, 12.2% and 16.9% at the depth of 1.7mm, and 5.7% and 5.4 % at the depth of 3.5mm, respectively. It can be observed that the tangential and the axial stresses have approximately the same contribution on Von-Mises stress. Although there was a lower contribution of radial stress at deeper depths compared to the surface, it is still more prominent than axial and tangential stress. Therefore, it should be noted that the minimum MVMS is attained approximately when the radial compressive residual stress increases to an optimum value, irrespective of the type of two other components. However, a strong destructive influence of the superimposed radial residual stress was observed when it increases beyond the optimal value.

**Table 4**  
Optimal parameters of initial residual stress components and optimized MVMS.

|         | Optimal parameters (MPa) |                   |              | Optimized $\sigma_{VM}$ (MPa) |
|---------|--------------------------|-------------------|--------------|-------------------------------|
|         | Radial stress            | Tangential stress | Axial stress |                               |
| Surface | -552.1                   | -110.2            | -100.9       | 458.7                         |
| 1.7mm   | -382.1                   | -118.1            | -95.1        | 290.9                         |
| 3.5mm   | -356.9                   | -268.7            | -255.2       | 147.2                         |

**Table 5**  
Summary of ANOVA results.

| Source         | DF  | Surface contribution (%) | 1.7mm Contribution (%) | 3.5mm Contribution (%) | P-Value |
|----------------|-----|--------------------------|------------------------|------------------------|---------|
| A (Radial)     | 5   | 63.7                     | 55.1                   | 24.8                   | <0.001  |
| B (Tangential) | 5   | 14.8                     | 12.2                   | 5.7                    | <0.001  |
| C (Axial)      | 5   | 18.1                     | 16.9                   | 5.4                    | <0.001  |
| AB             | 25  | 0.7                      | 5.5                    | 10.6                   | <0.001  |
| AC             | 25  | 0.69                     | 6.5                    | 19.23                  | <0.001  |
| BC             | 25  | 1.46                     | 2.5                    | 10.8                   | <0.001  |
| Error          | 125 | 0.43                     | 1.0                    | 23.1                   |         |
| Total          | 215 |                          |                        |                        |         |

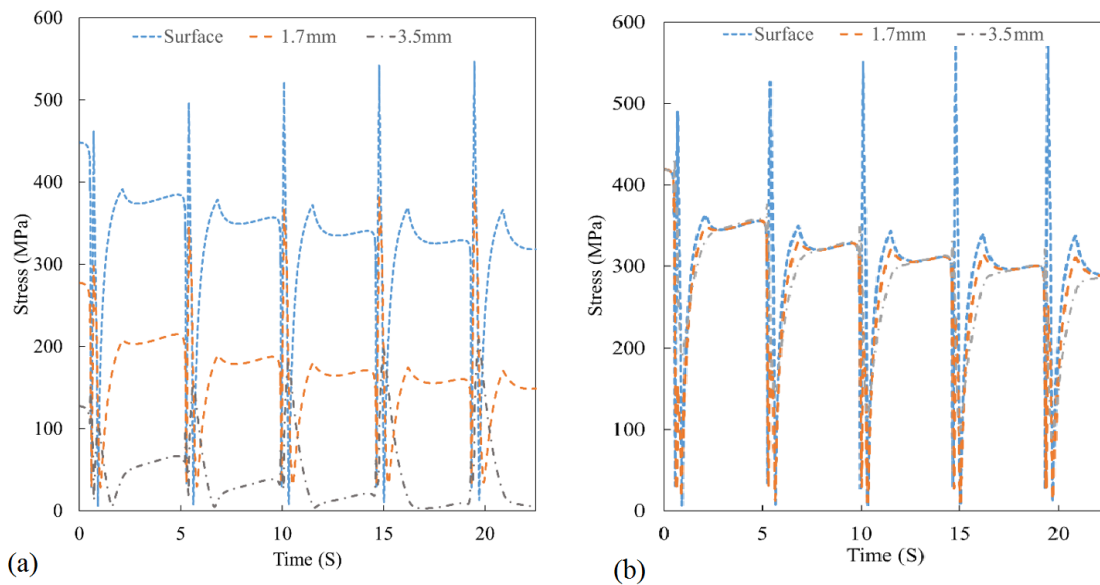


**Fig. 5.** a) Optimized Von-Mises stresses evolution history within different depths; b) Multi-objective uniform optimized Von-Mises stresses evolution history through the depth up to 3.5mm.

**Table 6**

Multi-objective optimal parameters of initial residual stress components and optimized MVMS.

|           | Input optimal parameters (MPa) |                   |              | Multi-objective of optimized maximum $\sigma_{VM}$ (MPa) |        |        |
|-----------|--------------------------------|-------------------|--------------|--|--------|--------|
|           | Radial stress                  | Tangential stress | Axial stress | Surface  | 1.7mm  | 3.5mm  |
| 0 - 3.5mm | -575.058                       | -162.109          | -152.804     | 471.45   | 414.86 | 447.47 |

Fig. 5a shows the optimized Von-Mises stresses obtained in the presence of optimal residual stresses during the first revolution. Comparing Figs. 5a and 4d, demonstrates that the MVMS on the surface is reduced significantly from 909 to 458.7 by introducing optimal initial residual stress. A similar effect at the depth of 1.7mm and 3.5mm can be seen. The optimal initial residual stress decreases the magnitude of MVMS to 290.9MPa from 670.8MPa at the depth of 1.7mm. Also, the magnitude of MVMS at the depth of 3.5mm decreases to 147.2MPa from 334.6MPa. The consequence of these reductions will lead to a significant reduction of micro-scale plasticity and near-inclusion micro cracks [3].

Despite the simplicity of the theory of proposing the optimal residual stresses in different points, there are practical limitations when applying it to real applications. Shot peening and heat treatment are two well-known processes, which can induce compressive residual stresses into the subsurface of materials in order to improve the fatigue life [26]. However, it is worth noting that future works are needed to find a method for implementing desired residual stress components at different points in different directions. In addition, the rapid changing of applying optimized Von-Mises stress between different points could be a cause of the

possibility of additional negative effects on fatigue life. Therefore, in this paper, the ANN method and multi-objective GA optimization algorithm were also used to find the optimal value of initial components of residual stresses through the entire length of a thin subsurface layer up to 3.5mm, which results in minimizing the maximum value of a constant Von-Mises stress. The results were reported in Table 6 and Fig. 5b. As can be seen, the optimized Von-Mises stress is equal to 471.45MPa on the surface, 414.86MPa at the depth of 1.7mm, and 447.47MPa at 3.5mm. Therefore, it can be concluded from Fig. 5b that with superimposing the optimal residual stresses in Table 6, the MVMS is observed to a constant optimized level around 450MPa through the thin layer under the surface.

#### 4. Conclusions

Prior works have documented the effectiveness of imposing initial compressive residual stress in reducing the MVMS and improving the fatigue life of bearings. However, these studies either have been mechanical or have not focused on finding the optimal value of initial residual stress in different components of stress tensors in order to find the best-optimized values. In this paper, a semi-analytical method was proposed to opti-

mize residual stress in three directions, aiming to minimize the MVMS of work roll during hot rolling. The results of the current study can be summarized as follows:

1. Considering the initial residual stress, radial residual stress was the most effective parameter on the Von-Mises stress. Axial and tangential stresses have the same contribution from an effectiveness point of view on the MVMS.
2. By proposing the optimal value of initial compressive residual stress components at three directions, MVMS of the work roll was reduced by 48.6 % on the surface, 47.93% at 1.7mm and 33.48 % at 3.5mm during hot rolling based on proposing a semi-analytical model and ANN method and Genetic algorithm optimization.
3. Analysis of attained optimal residual stresses for three depths revealed that the subsurface of the work roll experienced a rapid change of optimal residual stresses and optimized Von-Mises stresses, which is out of access from a practical point of view. Thus, the MVMS reached a minimized level of around 450MPa with proposing uniform optimal residual stresses through a thin layer near the surface using multi-objective Genetic algorithm optimization.
4. Besides the attained lower MVMS under cyclic thermo-mechanical loading, the Von-Mises amplitude was reduced significantly, which resulted in the lower fatigue crack initiation and propagation.

## References

- [1] S. Spuzic, K.N. Strafford, C. Subramaniana, G. Savageb, *Wear of hot rolling mill rolls: an overview*, *Wear*, 176(2) (1994) 261-271.
- [2] P.G. Stevens, K.P. Ivens, P. Harper, *Increasing work-roll life by improved roll cooling practice*, *J. Iron and Steel Inst.*, 209(1) (1971) 1-11.
- [3] H. Mahdavi, K. Poullos, C.F. Niordson, *Effect of superimposed compressive stresses on rolling contact fatigue initiation at hard and soft inclusions*, *Int. J. Fatigue*, 134 (2020) 105399.
- [4] F.J. Belzunce, A. Ziadi, C. Rodriguez, *Structural integrity of hot strip mill rolling rolls*, *Eng. Fail. Anal.*, 11(1) (2004) 789-797.
- [5] F. Weidlich, A.P.V. Braga, L.G.D.B. da Silva Lima, M.B. Júnior, R.M. Souza, *The influence of rolling mill process parameters on roll thermal fatigue*, *Int. J. Adv. Manuf. Technol.*, 102 (2019) 2159-2171.
- [6] A.P. Voskamp, E.J. Mittemeijer, *The effect of the changing microstructure on the fatigue behavior during cyclic rolling contact loading*, *Int. J. Mater. Res.*, 88(4) (1997) 310-320.
- [7] N.G. Popinceanu, E. Diaconescu, S. Cretu, *Critical stresses in rolling contact fatigue*, *Wear*, 71(3) (1981) 265-282.
- [8] A. Warhadpande, F. Sadeghi, R.D. Evans, M.N. Kotzalas, *Influence of plasticity-induced residual stresses on rolling contact fatigue*, *Tribol. Trans.*, 55(4) (2012) 422-37.
- [9] E.V. Zaretsky, R.J. Parker, W.J. Anderson, *A study of residual stress induced during rolling*, *J. Lubr. Technol.*, 91(2) (1969) 314-318.
- [10] K. Hu, F. Zhu, J. Chen, N.-A., Noda, W. Han, Y. Sano, *Simulation of thermal stress and fatigue life prediction of high speed steel work roll during hot rolling considering the initial residual stress*, *Metals*, 9(9) (2019) 966.
- [11] K. Hu, Q. Shi, W. Han, F. Zhu, J. Chen, *On the evolution of temperature and combined stress in a work roll under cyclic thermo-mechanical loadings during hot strip rolling and idling*, *Materials*, 13(21) (2020) 5054.
- [12] Sp.S. Cretu, N.G. Popinceanu, *The influence of residual-stresses induced by plastic deformation on rolling-contact fatigue*, *Wear*, 105 (1985) 153-170.
- [13] H. Mahdavi, K. Poullos, Y. Kadin, C.F. Niordson, *Finite element study of cyclic plasticity near a subsurface inclusion under rolling contact and macro-residual stresses*, *Int. J. Fatigue*, 143 (2021) 105981.
- [14] C.S. Li, X.H. Liu, G.D. Wang, X.M. He, *Three-dimensional FEM analysis of work roll temperature field in hot strip rolling*, *J. Mater. Sci. Technol.*, 18(10) (2002) 1147-1150.
- [15] J.D. Lee, M.T. Manzari, Y.L. Shen, W. Zeng, *A finite element approach to transient thermal analysis of work rolls in rolling process*, *J. Manuf. Sci. Eng.*, 122(4) (2000) 706-716.
- [16] D. Benasciutti, E. Brusa, G. Bazzaro, *Finite elements prediction of thermal stresses in work roll of hot rolling mills*, *Procedia Eng.*, 2(1) (2010) 707-716.
- [17] D. Benasciutti, *On thermal stress and fatigue life evaluation in work rolls of hot rolling mill*, *J. Strain Anal. Eng. Des.*, 47(5) (2012) 297-312.

- [18] G.Y. Deng, H.T. Zhu, A.K. Tieu, L.H. Su, M. Reid, L. Zhang, P.T. Wei, X. Zhao, H. Wang, J. Zhang, J.T. Li, T.D. Ta, Q. Zhu, C. Kong, Q. Wu, Theoretical and experimental investigation of thermal and oxidation behaviors of a high speed steel work roll during hot rolling, *Int. J. Mech. Sci.*, 131-132 (2017) 811-826.
- [19] G.Y. Deng, Q. Zhu, K. Tieu, H.T. Zhu, M. Reid, A.A. Saleh, L.H. Su, T.D. Ta, J. Zhang, C. Lu, Q. Wu, D.L. Sun, Evolution of microstructure, temperature and stress in a high speed steel work roll during hot rolling: Experiment and modelling, *J. Mater. Process. Technol.*, 240 (2017) 200-208.
- [20] Simulia ABAQUS 6.11. ABAQUS Analysis User's Manual. HKS Inc., Providence, RI, USA, (2011).
- [21] S. Shida, Empirical formula of flow stress of carbon steels resistance to deformation of carbon steels at elevated temperature, *Journal of the Japan Society for Technology of Plasticity*, 10(103) (1969) 610-617.
- [22] R.B. Sims, The calculation of roll force and torque in hot rolling mills, *Proc. Inst. Mech. Eng.*, 168(1) (1954) 191-200.
- [23] N.A. Noda, K. Hu, Y. Sano, K. Ono, Y. Hosokawa, Residual stress simulation for hot strip bimetallic roll during quenching, *Steel Res. Int.*, 87(11) (2016) 1478-1488.
- [24] N.A. Noda, Y. Sano, M. Radzi Aridi, K. Tsuboi, N. Oda, Residual stress differences between uniform and non-uniform heating treatment of bimetallic roll: Effect of creep behavior on residual stress, *Metals*, 8 (2018) 952.
- [25] A. Melander, M. Larsson, The effect of stress amplitude on the cause of fatigue crack initiation in a spring steel, *Int. J. Fatigue*, 15(2) (1993) 119-131.
- [26] S. Aguado-Montero, J. Vázquez, C. Navarro, J. Domínguez, Optimal shot peening residual stress profile for fatigue, *Theor. Appl. Fract. Mech.*, 116 (2021) 103109.